Robust Drone Detection and Classification from Radio Frequency Signals using Convolutional Neural Networks

Stefan Glüge[1] [a], Matthias Nyfeler[1] [b], Nicola Ramagnano[2], Claus Horn[1] [c], and Christof Schüpbach[3] [d]

[1]*Institute of Computational Life Sciences, Zurich University of Applied Sciences, 8820 Wädenswil, Switzerland*

[2]*Institute for Communication Systems, Eastern Switzerland University of Applied Sciences, 8640 Rapperswil-Jona, Switzerland*

[3]*armasuisse Science + Technology, 3602 Thun, Switzerland*

{*stefan.gluege, matthias.nyfeler, claus.horn*}*@zhaw.ch, nicola.ramagnano@ost.ch, christof.schuepbach@armasuisse.ch*

Abstract: As the number of unmanned aerial vehicles (UAVs) in the sky increases, safety issues have become more pressing. In this paper, we compare the performance of convolutional neural networks (CNNs) using first, 1D in-phase and quadrature (IQ) data and second, 2D spectrogram data for detection and classification of UAVs based on their radio frequency (RF) signals. We focus on the robustness of the models to low signal-to-noise ratios (SNRs), as this is the most relevant aspect for a real-world application. Within an input type, either IQ or spectrogram, we found no significant difference in performance between models, even as model complexity increased. In addition, we found an advantage in favor of the 2D spectrogram representation of the data. While there is basically no performance difference at SNRs ≥ 0 dB, we observed a 100% improvement in balanced accuracy at -12 dB, i.e. 0.842 on the spectrogram data compared to 0.413 on the IQ data for the VGG11 model. Together with an easy-to-use benchmark dataset, our findings can be used to develop better models for robust UAV detection systems.

1 INTRODUCTION

Drones, or civil UAVs, have evolved from hobbyist toys to commercial systems with many applications. As more drones fly in the sky, safety issues are becoming more pressing. Regulations and technical solutions (such as transponder systems) are needed to safely integrate UAVs into the airspace. However, even with a standard airspace integration, drones can still pose serious threats. Safety regulations can be circumvented by technical and human error or deliberate misuse. To protect critical infrastructure such as airports, drone detection and classification systems are needed that do not depend on the cooperation of the UAV. Various technologies such as audio, video, radar, or RF scanners have been proposed for this task (Kunze and Saha, 2022).

In this paper, we investigate different approaches for the detection and classification of drones based on their RF signals. We compare the performance of CNNs using two different representations of the input data: first, raw IQ data, without requiring much preprocessing (except for windowing and normalization) and second, spectrogram data computed with consecutive Fourier transforms for the real and imaginary parts of the signal. In terms of performance, we focus on the robustness of the models to low SNRs, as this is the most relevant aspect for a real-world application of the system. To facilitate future model development, we provide an easy-to-use benchmark dataset.

In the next section, we briefly review related work in this research area, followed by a description of the data collection and data preprocessing procedure in Section 2. Section 3 describes the model architectures and their training/validation method. The resulting performance metrics are presented in Section 4 and further discussed in Section 5.

---

[a] https://orcid.org/0000-0002-7484-536X
[b] https://orcid.org/0000-0001-7929-7625
[c] https://orcid.org/0000-0003-1557-7913
[d] https://orcid.org/0000-0001-5822-3360

1.1 Related Work

A literature review of machine learning (ML) approaches for drone detection and classification that refelcts the state of the art in 2019, is provided by Taha and Shoufan (Taha and Shoufan, 2019). The authors provide an overview of approaches for radar, visual data, acoustic data, and RF-based systems. Therefore, we briefly describe how the field has evolved since 2019 and reassess our use case, namely RF data in a noisy environment.

The openly available DroneRF dataset (Allahham et al., 2019) has been used in several works (Al-Sa'd et al., 2019; Swinney and Woods, 2020; Zhang, 2021). It contains RF recordings from three drones in four flight modes (i.e., on, hovering, flying, video recording). It was recorded using universal software radio peripheral (USRP) software-defined radio (SDR) transceivers. Signals that could be considered noise in the 2.4 GHz band (Bluetooth, Wi-Fi) were not recorded. Furthermore, the dataset contains only time series data, and not the complex IQ signals.

Together with the dataset, the authors proposed three deep neural networks to detect the presence of a drone, the presence of a drone and its type, and the presence of a drone, its type, and its flight mode. The average accuracy is reported to be 99.7% for the 2-class problem, 84.5% for the 4-class problem, and 46.8% for the 10-class problem, respectively (Al-Sa'd et al., 2019).

Medaiyese et al. (Medaiyese et al., 2021) propose a semi-supervised framework for UAV detection using wavelet analysis. Accuracy between 86% and 97% was achieved at SNRs of 30 dB and 18 dB, while it dropped to chance level for SNRs below 10 dB to 6 dB. They recorded a dataset consisting of six different types of drones, as well as two Bluetooth devices and two Wi-Fi devices. Unfortunately, this dataset is not openly available.

The openly available DroneDetect_V2 dataset was created by Swinney and Woods (Swinney and Woods, 2021). It contains raw IQ data recorded with a BladeRF SDR. Seven drone models were recorded in three different flight modes (on, hovering, flying). Measurements were also repeated with different types of noise, such as interference from a Bluetooth speaker, a Wi-Fi hotspot, and simultaneous Bluetooth and Wi-Fi interference. The dataset does not include measurements without drones, which would be necessary to evaluate a drone detection system. The results in (Swinney and Woods, 2021) show that Bluetooth signals are more likely to interfere with detection and classification accuracy than Wi-Fi signals. Overall, frequency domain features extracted from a

Figure 1: Recording of drone signals in the anechoic chamber. A DJI Phantom 4 Pro drone with the DJI Phantom GL300F remote control.

CNN where shown to be more robust than time domain features in the presence of interference.

Unlike most deep learning approaches, Ge et al. (Ge et al., 2021) focus on pre-processing and combining signals from two frequency bands before feeding them into a neural network classifier to improve classification accuracy, which is reported to improve from 46.8% to 91.9%.

Zhang et al. (Zhang et al., 2023) used downlink video data and focused on data augmentation with various environmental signals. They applied data segmentation techniques of spectral features with a ResNet architecture for the RF data with a bandwidth of 100 MHz with SNRs ranging from 20 dB down to 0 dB. The accuracy at the lowest SNR of 0 dB was still around 70%.

2 MATERIALS

2.1 Data Acquisition

To record pure drone signals without any interference, the drone remote control and, if present, the drone itself were placed inside the anechoic chamber, see Figure 1. The signals were received by a LogPer antenna and sampled and stored by an Ettus Research USRP B210. In the static measurement, the respective signals of the remote control (TX) alone or with the drone (RX) were measured. In the dynamic measurement, one person at a time was inside the anechoic chamber and operated the remote control (TX) to generate a signal that is as close to reality as possible. All signals were recorded at a sampling frequency of 56 MHz (highest possible real-time bandwidth). All drone models with recording parameters are listed in Table 1, including both uplink and downlink signals.

To access the robustness of a drone detection model, we further considered three types of noise

Table 1: Transmitters and receivers recorded in the dataset and their respective labels. Additionally, we show the class label used, the center frequency (GHz), the channel spacing (MHz), the burst duration (ms), and the repetition period of the respective signals (ms).

Transmitter	Receiver	Label	Center Freq.	Spacing	Duration	Repetition
DJI Phantom GL300F	DJI Phantom 4 Pro	DJI	2.44175	1.7	2.18	630
Futaba T7C	-	FutabaT7	2.44175	2	1.7	288
Futaba T14SG	Futaba R7008SB	FutabeT14	2.44175	3.1	1.4	330
Graupner mx-16	Graupner GR-16	Graupner	2.44175	1	1.9/3.7	750
Bluetooth/Wi-Fi Noise	-	Noise	2.44175			
Taranis ACCST	X8R Receiver	Taranis	2.440	1.5	3.1/4.4	420
Turnigy 9X	-	Turnigy	2.445	2	1.3	61, 120-2900

and interference. First, Bluetooth/Wi-Fi noise was recorded using the hardware setup described above. The measurements were performed in a public and busy university building. In this open recording setup, we had no control over the exact number or types of active Bluetooth/Wi-Fi devices and the actual traffic in progress.

Second, artificial white Gaussian noise was used, and third, receiver noise from the USRP was used at various gain settings without the antenna attached. This should prevent the final model from misclassifying quantization noise in the absence of a signal, especially at low gain settings.

2.2 Data Preparation

To reduce memory consumption and computational effort, we reduced the bandwidth of the signals by downsampling from 56 MHz to 14 MHz using the SciPy (Virtanen et al., 2020) signal.decimate function with an 8th order Chebyshev type I filter.

The drone signals come in short bursts with some low power gain or background noise in between. For training purposes, we divided the signals into vectors of 16384 samples (≈ 1.2 ms). Only vectors containing a burst, or at least a partial burst, were considered for training. This was achieved by applying an energy threshold as shown in Figure 2.

The selected drone signal vectors x with $i \in \{1, \dots k\}$ were normalized to a carrier power of 1 per sample, i.e. only the part of the signal vector containing drone bursts was considered for the power calculation (m samples out of k). This was achieved by identifying the bursts as the samples where a smoothed energy was above a threshold, as shown in Figure 3. The signal vectors x are thus normalized by

$$\hat{x}(i) = x(i) \ / \ \sqrt{\frac{1}{m} \sum_i |x(i)|^2}. \quad (1)$$

Noise vectors (Bluetooth, Wi-Fi, Amplifier, Gauss) n with samples $i \in \{1, \dots k\}$ were normalized
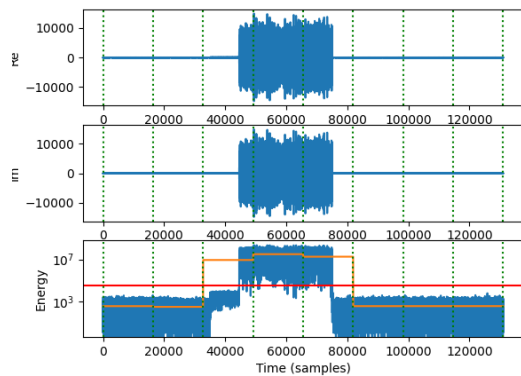

Figure 2: 10ms signal drone signal from DJI PhantomPro4 showing a signal burst. Only the vectors with average energy (orange) above the threshold (red) were used for training. The start/end of the considered vectors of 16384 samples are shown as green dashed lines. The large y-values are due to the not yet normalized raw int16 data.

to a mean power of 1 using

$$\hat{n}(i) = n(i) / \sqrt{\frac{1}{k} \sum_i |n(i)|^2}. \quad (2)$$

To train robust models, we mixed the drone signal vectors with noise at different SNRs. Since the signal carrier power and the noise power were both normalized to 1, we added separate normalized noise vectors $\hat{n}$, not considered in the noise class in the training dataset, to each normalized signal vector $\hat{x}$ as

$$\hat{y}(i) = \frac{\left(\sqrt{k} \cdot \hat{x}(i) + \hat{n}(i)\right)}{\sqrt{k+1}}, \text{ with } k = 10^{\text{SNR}/10}, \quad (3)$$

to generate the normalized vectors y at different SNRs used for training and validation.

Given the mixed normalized IQ vectors, we computed the spectrograms using the ScyPi signal.sepctrogram function with a Tukey window. Often only the absolute values of the spectrum are used, but in this study the full complex spectrum was considered to preserve phase information.
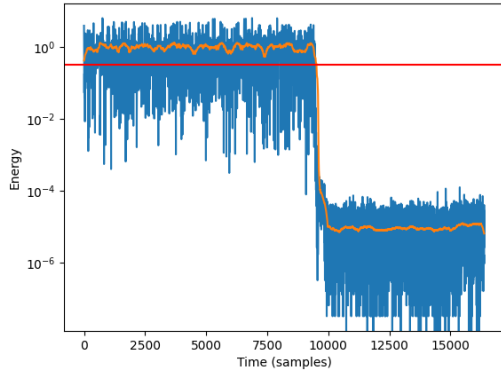
Figure 3: Drone signal vector with carrier normalization. Only those samples whose smoothed energy (orange) is above the threshold (red) are used for the normalization.

2.3 Benchmark Dataset

To facilitate future model development, we provide an easy-to-use benchmark dataset[1] together with a code example to get started[2]. The dataset consists of the non-overlapping signal vectors of length 16384, which corresponds to $\approx 1.2\,\text{ms}$ at $14\,\text{MHz}$. We also added Labnoise (Bluetooth, Wi-Fi, Amplifier) and Gaussian noise to the dataset.

After normalization, the drone signals were mixed with either Labnoise (50%) or Gaussian noise (50%). The noise class was created by mixing Labnoise and Gaussian noise in all possible combinations (i.e., Labnoise + Labnoise, Labnoise + Gaussian noise, Gaussian noise + Labnoise, and Gaussian noise + Gaussian noise). For the drone signal classes, as for the noise class, the number of samples for each level of SNR is evenly distributed over the interval of SNRs $\in [-20, 30]\,\text{dB}$ in steps of $2\,\text{dB}$, i.e., 3792-3800 samples per SNR level. The resulting number of samples per class is shown in Table 2.

After data normalization and mixing, we computed the power spectrum of each sample with consecutive Fourier transforms with non-overlapping segments of length 128 for the real and imaginary parts of the signal. That is, the two IQ signal vectors ($[2 \times 16384]$) are represented as two matrices ($[2 \times 128 \times 128]$). Figure 4 shows four samples of the data set for different types of drones at different SNRs.

---

3 METHODS

3.1 Model Architecture and Training

We tested different configurations of the Visual Geometry Group (VGG) CNN architecture (Simonyan and Zisserman, 2015). The main idea of this architecture is to use multiple layers of small (3×3) convolutional filters instead of larger ones. This is intended to increase the depth and expressiveness of the network, while reducing the number of parameters. The VGG architecture consists of several variants, such as VGG11 to VGG19, which differ in the number of convolutional layers (11 and 19, respectively). The VGG architecture achieves state-of-the-art results on the ImageNet (Deng et al., 2009) dataset, which contains 14 million images belonging to 1000 classes, and outperforms many previous models, such as AlexNet (Krizhevsky et al., 2012) and ZF-Net (Zeiler and Fergus, 2014). In addition to image classification, the architecture is also widely used as a feature extractor for other computer vision tasks such as object detection, face recognition (Parkhi et al., 2015), and semantic segmentation (Long et al., 2015).

To be able to process 1D IQ data, we adapted the VGG architecture from using Conv2D layers to Conv1d, MaxPool2d to MaxPool1d, and AdaptiveAvgPool2d to AdaptiveAvgPool1d, respectively. For the spectrogram input data the VGG architecture can be used as is. For the dense classification layer, we used 256 linear units followed by 7 linear units at the output (one unit per class).

For network training, we used a stratified 5-fold train-validation-test split. In each fold, we trained a network using 80% and 20% of the available samples for each class for training and testing, respectively. Repeating the stratified split five times ensures that each sample was in the test set once in each experiment. Within the training set, 20% of the samples were used as the validation set during training.

Model training was performed for 25 epochs with a batch size of 64. PyTorch's (Paszke et al., 2019) implementation of stochastic gradient descent optimization (Bottou, 1999) was used with a fixed momentum of 0.9. In addition, we applied a learning rate decay by a factor of 0.1 if the validation loss did not improve within the last 3 epochs of training. The initial learning rate was set to 0.005.

3.2 Model Evaluation

After each training epoch, the model was evaluated on the validation set. The model with the highest balanced accuracy was then saved and later evaluated on

Table 2: Number of samples in the different classes in the benchmark dataset.

Class	DJI	FutabaT14	FutabaT7	Graupner	Taranis	Turnigy	Noise
#samples	2194	6938	3661	6481	16546	10333	52552

(a) Turnigy at SNR 22 dB

(b) FutubaT14 at SNR 0 dB
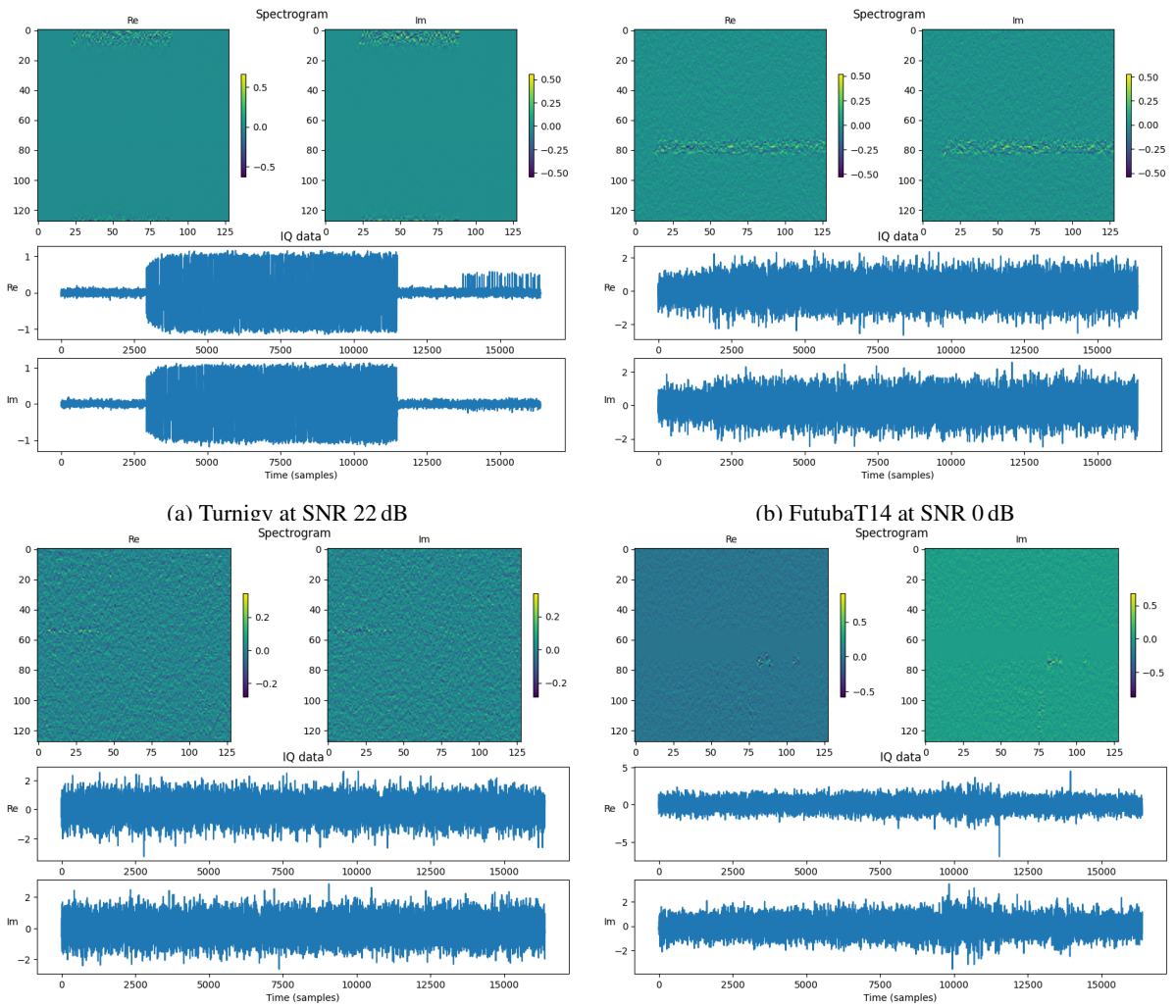
(c) DJI at SNR −12 dB

(d) Noise at SNR 6 dB

Figure 4: Spectrogram and IQ data samples from the benchmark dataset for different drones at different SNRs (a-c) and noise (d)

the withheld test data. The performance of the models on the test data was evaluated in terms of classification accuracy and balanced accuracy.

Accuracy is the simplest metric, measuring the proportion of correct predictions out of the total number of observations. It is simply calculated as the number of correct classifications divided by the total number of samples. However, accuracy can be misleading if the data is unbalanced. In our case, the noise class is overrepresented in the dataset (see Table 2).

Balanced accuracy is defined as the average of the recall obtained for each class, i.e. it gives equal weight to each class regardless of how frequent or rare it is.
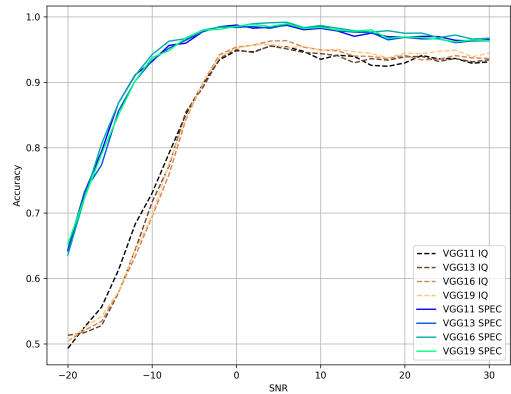
4 RESULTS

Table 3 shows the mean $\pm$ standard deviation of accuracy and balanced accuracy on the test data, obtained in the 5-fold cross-validation of the different models. The models using the IQ data at the input consistently perform 10% worse than those using the spectrogram data.

Within an input type, either IQ or spectrogram, there is no significant difference in performance between the models, even as the model complexity increases from VGG11 to VGG19.

The number of epochs for training (#epochs) shows when the highest balanced accuracy was reached in the validation. It can be seen that the less complex models (e.g. VGG11) need more time/epochs compared to the more complex models. However, the resulting classification performance is the same.

To further assess the robustness of the models to noise, we computed the accuracy and balance accuracy separately for each noise level in the dataset. Figure 5 shows the resulting 5-fold mean (balanced) accuracy over SNRs $\in [-20, 30]$ dB in 2 dB steps. Note that we do not show the standard deviation to keep the plots readable. In general, we observe a degradation in performance from 0 dB down to near chance level at -20 dB. At the lowest SNR level, we observe a large difference between the accuracy and the balanced accuracy. For example, about 0.65 for accuracy and 0.3 for balanced accuracy, for models trained on the spectrogram data. The reason for this is the overrepresentation of the noise class in the dataset, together with the fact that the vast majority of misclassifications occur between noise and drones and not between different types of drones. Figure 6 shows the confusion matrix for the VGG11 model with spectrogram data (VGG11 SPEC) at SNR -20 dB for a sin-

(a)
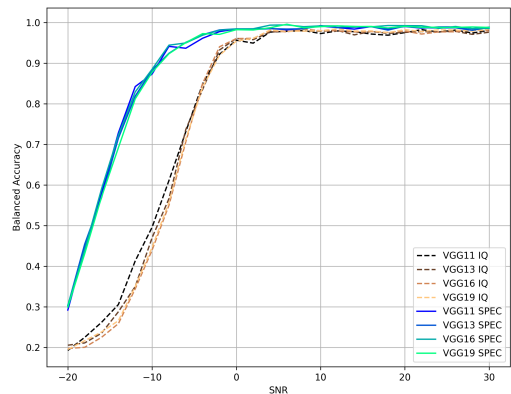
(b)

Figure 5: Mean accuracy a) and balanced accuracy b) obtained in the 5-fold cross-validation of the different models on the drone classification task over the SNR. The different types of input data are shown as solid lines for spectrogram (SPEC) and dashed lines for IQ.

gle validation on the test data. It illustrates the fact that the model mainly misclassifies drone signals as noise, which is to be expected at such a low SNR.

To access the spread of the results at low SNR levels, we show the 5-fold mean $\pm$ standard deviation of accuracy and balanced accuracy in Tables 4 and 5 for SNR 0 dB, -6 dB, -12 db, and -18 dB.

5 DISCUSSION

In our experiment, we saw a significant advantage in favor of the 2D spectrogram representation of the data over the 1D IQ representation. While there is no performance gap at SNRs ≥ 0 dB, we observed a huge difference at lower SNRs (see Figure 5). For example

Table 3: Mean ± standard deviation of the accuracy (Acc.) and the balanced accuracy (balanced Acc.) obtained in 5-fold cross-validation of the different models in the drone classification task for different types of input data, i.e. spectrogram (SPEC) and IQ. The best result is highlighted. An indication of the model training time is given with the mean ± standard deviation of the number of training epochs (#epochs). The number of trainable parameters (#params) indicates the complexity of the model.

Input	Model	Acc.	balanced Acc.	#epochs	#params
IQ	VGG11	0.911 ± 0.026	0.790 ± 0.005	26.6 ± 0.800	$3.47 \cdot 10^6$
	VGG13	0.906 ± 0.031	0.784 ± 0.004	22.8 ± 4.354	$3.53 \cdot 10^6$
	VGG16	0.893 ± 0.023	0.780 ± 0.009	23.4 ± 2.871	$5.30 \cdot 10^6$
	VGG19	0.911 ± 0.037	0.783 ± 0.005	23.4 ± 5.426	$7.07 \cdot 10^6$
SPEC	VGG11	0.981 ± 0.012	0.900 ± 0.005	20.4 ± 3.072	$9.35 \cdot 10^6$
	VGG13	0.981 ± 0.008	0.897 ± 0.004	16.2 ± 2.135	$9.54 \cdot 10^6$
	VGG16	0.988 ± 0.002	0.899 ± 0.005	17.8 ± 1.720	$14.85 \cdot 10^6$
	VGG19	0.989 ± 0.005	0.898 ± 0.003	17.4 ± 0.800	$20.16 \cdot 10^6$

Table 4: Mean ± standard deviation of the **accuracy** obtained in 5-fold cross-validation of the different models in the drone classification task for different types of input data, i.e. spectrogram (SPEC) and IQ, at different noise levels.

SNR		0 dB	−6 dB	−12 dB	−18 dB
Input	Model				
IQ	VGG11	0.948 ± 0.006	0.851 ± 0.017	0.683 ± 0.017	0.526 ± 0.010
	VGG13	0.950 ± 0.006	0.856 ± 0.011	0.644 ± 0.027	0.517 ± 0.009
	VGG16	0.954 ± 0.010	0.843 ± 0.015	0.634 ± 0.025	0.521 ± 0.024
	VGG19	0.952 ± 0.005	0.845 ± 0.009	0.642 ± 0.018	0.525 ± 0.012
SPEC	VGG11	0.987 ± 0.003	0.960 ± 0.007	0.911 ± 0.010	0.732 ± 0.006
	VGG13	0.984 ± 0.005	0.964 ± 0.010	0.902 ± 0.016	0.733 ± 0.017
	VGG16	0.985 ± 0.006	0.967 ± 0.010	0.910 ± 0.006	0.724 ± 0.011
	VGG19	0.985 ± 0.002	0.968 ± 0.006	0.902 ± 0.016	0.723 ± 0.028

Table 5: Mean ± standard deviation of the **balanced accuracy** obtained in the 5-fold cross-validation of the different models in the drone classification task for different types of input data, i.e. spectrogram (SPEC) and IQ, at different noise levels.

| SNR		0 dB	−6 dB	−12 dB	−18 dB
Input	Model				
IQ	VGG11	0.956 ± 0.006	0.731 ± 0.028	0.413 ± 0.012	0.225 ± 0.015
	VGG13	0.961 ± 0.012	0.737 ± 0.041	0.350 ± 0.025	0.211 ± 0.009
	VGG16	0.960 ± 0.006	0.706 ± 0.044	0.344 ± 0.043	0.201 ± 0.019
	VGG19	0.954 ± 0.009	0.713 ± 0.024	0.350 ± 0.023	0.217 ± 0.016
SPEC	VGG11	0.984 ± 0.009	0.937 ± 0.006	0.842 ± 0.035	0.444 ± 0.027
	VGG13	0.985 ± 0.005	0.951 ± 0.012	0.819 ± 0.036	0.454 ± 0.001
	VGG16	0.984 ± 0.007	0.950 ± 0.014	0.829 ± 0.020	0.441 ± 0.032
	VGG19	0.983 ± 0.006	0.951 ± 0.006	0.812 ± 0.021	0.431 ± 0.023
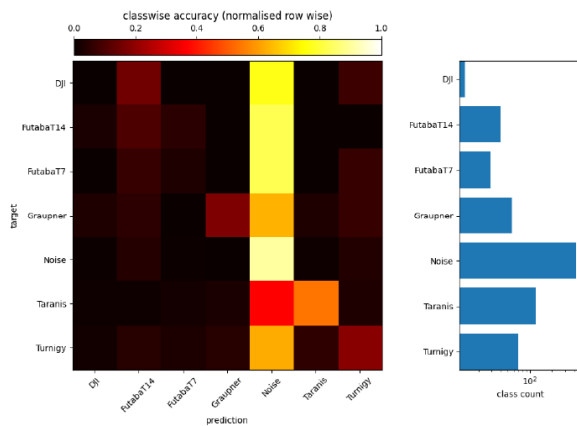
Figure 6: Confusion matrix of a run of the VGG11 model with spectrogram data at the input (VGG11 SPEC) at SNR -20 dB. The average accuracy is 0.63 and the average balanced accuracy is 0.28.

at -12 dB, there is still a decent balanced accuracy of 0.842 on the spectrogram data compared to 0.413 on the IQ data for the VGG11 model (see Table 5).

The obvious question is why the spectrogram representation seems to be easier to separate in noisy conditions. Part of the explanation may lie in the basic architecture of the VGG model. It was originally developed for image classification tasks, so it should not be surprising that it is better suited to the problem of 2D spectrogram data compared to 1D IQ data. However, given the complexity of the models, one might assume that they can learn the necessary features from 1D representations. Apparently, in our case, this assumption only holds true for SNRs≥ 0.

Since drones have a much narrower bandwidth than noise, one might expect them to be easier to detect in frequency space. However, Fourier transforming the IQ vectors (16384 samples) did not give better performance at SNRs< 0 dB. This confirms the assumption that a deep CNN can learn the necessary filters for a Fourier transform. However, the combined time- and frequency-domain information in the spectrogram seems to help the network focus on both frequency information and the temporal structure of the signal bursts.

Given our benchmark dataset, it is possible to optimize the model side of the problem and perhaps find a model architecture with comparable or better performance using the IQ data, for example with neural architecture search approaches (Chen et al., 2018).

Furthermore, we have seen that the confusion at low SNRs mainly occurs between the noise class and the drones, and not between the different drones themselves (see Figure 6). This is particularly relevant for the application of drone detection systems in security sensitive areas. The first priority is to detect any kind of UAV, regardless of its type. Since it seems to be comparatively easy to learn the class separation at high SNRs, one can shift the focus during learning by redistributing the samples towards lower SNRs instead of the equal distribution we used.

Optimizing the data collection and preprocessing itself is beyond the scope of this work. The hardware setup was chosen for the development of a rather simple and low-budget drone detection system (consumer grade notebook with GPU + SDR). Several parameters, such as sampling frequency, length of input vectors, etc., were set to allow real-time detection with a limited amount of memory and computing power. That is, data acquisition, preprocessing, and model inference should not take significantly longer than the signal being processed (≈ 1.2 ms per sample in our case).

REFERENCES

Al-Sa'd, M. F., Al-Ali, A., Mohamed, A., Khattab, T., and Erbad, A. (2019). Rf-based drone detection and identification using deep learning approaches: An initiative towards a large open source drone database. *Future Generation Computer Systems*, 100:86–97.

Allahham, M. S., Al-Sa'd, M. F., Al-Ali, A., Mohamed, A., Khattab, T., and Erbad, A. (2019). Dronerf dataset: A dataset of drones for rf-based detection, classification and identification. *Data in Brief*, 26:104313.

Bottou, L. (1999). *On-Line Learning and Stochastic Approximations*, pages 9–42. Cambridge University Press, USA.

Chen, L.-C., Collins, M. D., Zhu, Y., Papandreou, G., Zoph, B., Schroff, F., Adam, H., and Shlens, J. (2018). Searching for efficient multi-scale architectures for dense image prediction. In *Proceedings of the 32nd International Conference on Neural Information Processing Systems*, NIPS'18, page 8713–8724, Red Hook, NY, USA. Curran Associates Inc.

Deng, J., Dong, W., Socher, R., Li, L.-J., Li, K., and Fei-Fei, L. (2009). Imagenet: A large-scale hierarchical image database. In *2009 IEEE conference on computer vision and pattern recognition*, pages 248–255. Ieee.

Ge, C., Yang, S., Sun, W., Luo, Y., and Luo, C. (2021). For rf signal-based uav states recognition, is preprocessing still important at the era of deep learning? In *2021 7th International Conference on Computer and Communications (ICCC)*, pages 2292–2296.

Krizhevsky, A., Sutskever, I., and Hinton, G. E. (2012). Imagenet classification with deep convolutional neural networks. In Pereira, F., Burges, C., Bottou, L., and Weinberger, K., editors, *Advances in Neural Information Processing Systems*, volume 25. Curran Associates, Inc.

Kunze, S. and Saha, B. (2022). Drone classification with a

convolutional neural network applied to raw iq data. Institute of Electrical and Electronics Engineers Inc.

Long, J., Shelhamer, E., and Darrell, T. (2015). Fully convolutional networks for semantic segmentation. In *2015 IEEE Conference on Computer Vision and Pattern Recognition (CVPR)*, pages 3431–3440.

Medaiyese, O. O., Ezuma, M., Lauf, A. P., and Guvenc, I. (2021). Semi-supervised learning framework for uav detection. volume 2021-September, pages 1185–1190. Institute of Electrical and Electronics Engineers Inc.

Parkhi, O. M., Vedaldi, A., and Zisserman, A. (2015). Deep face recognition. In Xianghua Xie, Mark W. Jones, G. K. L. T., editor, *Proceedings of the British Machine Vision Conference (BMVC)*, pages 41.1–41.12. BMVA Press.

Paszke, A., Gross, S., Massa, F., Lerer, A., Bradbury, J., Chanan, G., Killeen, T., Lin, Z., Gimelshein, N., Antiga, L., Desmaison, A., Kopf, A., Yang, E., DeVito, Z., Raison, M., Tejani, A., Chilamkurthy, S., Steiner, B., Fang, L., Bai, J., and Chintala, S. (2019). Pytorch: An imperative style, high-performance deep learning library. In Wallach, H., Larochelle, H., Beygelzimer, A., d'Alché-Buc, F., Fox, E., and Garnett, R., editors, *Advances in Neural Information Processing Systems 32*, pages 8024–8035. Curran Associates, Inc.

Simonyan, K. and Zisserman, A. (2015). Very deep convolutional networks for large-scale image recognition. In Bengio, Y. and LeCun, Y., editors, *3rd International Conference on Learning Representations, ICLR 2015, San Diego, CA, USA, May 7-9, 2015, Conference Track Proceedings*.

Swinney, C. J. and Woods, J. C. (2020). Unmanned aerial vehicle flight mode classification using convolutional neural network and transfer learning. In *2020 16th International Computer Engineering Conference (ICENCO)*, pages 83–87.

Swinney, C. J. and Woods, J. C. (2021). Rf detection and classification of unmanned aerial vehicles in environments with wireless interference. pages 1494–1498. Institute of Electrical and Electronics Engineers Inc.

Taha, B. and Shoufan, A. (2019). Machine learning-based drone detection and classification: State-of-the-art in research. *IEEE Access*, 7:138669–138682.

Virtanen, P., Gommers, R., Oliphant, T. E., Haberland, M., Reddy, T., Cournapeau, D., Burovski, E., Peterson, P., Weckesser, W., Bright, J., van der Walt, S. J., Brett, M., Wilson, J., Millman, K. J., Mayorov, N., Nelson, A. R. J., Jones, E., Kern, R., Larson, E., Carey, C. J., Polat, İ., Feng, Y., Moore, E. W., VanderPlas, J., Laxalde, D., Perktold, J., Cimrman, R., Henriksen, I., Quintero, E. A., Harris, C. R., Archibald, A. M., Ribeiro, A. H., Pedregosa, F., van Mulbregt, P., and SciPy 1.0 Contributors (2020). SciPy 1.0: Fundamental Algorithms for Scientific Computing in Python. *Nature Methods*, 17:261–272.

Zeiler, M. D. and Fergus, R. (2014). Visualizing and understanding convolutional networks. In Fleet, D., Pajdla, T., Schiele, B., and Tuytelaars, T., editors, *Computer Vision – ECCV 2014*, pages 818–833, Cham. Springer International Publishing.

Zhang, H., Li, T., Li, Y., Li, J., Dobre, O. A., and Wen, Z. (2023). Rf-based drone classification under complex electromagnetic environments using deep learning. *IEEE Sensors Journal*, 23(6):6099–6108.

Zhang, Y. (2021). Rf-based drone detection using machine learning. In *2021 2nd International Conference on Computing and Data Science (CDS)*, pages 425–428.